Modulation of sarcoplasmic reticulum Ca^{2+} release by glycolysis in cat atrial myocytes

Jens Kockskämper, Aleksey V. Zima and Lothar A. Blatter

Department of Physiology, Stritch School of Medicine, Loyola University Chicago, 2160 South First Avenue, Maywood, IL 60153, USA

In cardiac myocytes, glycolysis and excitation–contraction (E–C) coupling are functionally coupled. We studied the effects of inhibitors (2-deoxy-D-glucose (2-DG), iodoacetate (IAA)), intermediates (glucose-6-phosphate (G6P), fructose-6-phosphate (F6P), fructose-1,6-bisphosphate (FBP), phosphoenolpyruvate (PEP)) and products (pyruvate, L-lactate) of glycolysis on sarcoplasmic reticulum (SR) Ca^{2+} release and uptake in intact and permeabilized cat atrial myocytes. In field-stimulated (0.5–0.7 Hz) intact myocytes, 2-DG (10 mM) and IAA (1 mM) caused elevation of diastolic $[Ca^{2+}]_i$ and $[Ca^{2+}]_i$ transient alternans (Ca^{2+} alternans) followed by a decrease of the amplitude of the $[Ca^{2+}]_i$ transient. Focal application of 2-DG resulted in local Ca^{2+} alternans that was confined to the region of exposure. 2-DG and IAA slowed the decay kinetics of the $[Ca^{2+}]_i$ transient and delayed its recovery (positive staircase) after complete SR depletion, suggesting impaired activity of the SR Ca^{2+}-ATPase (SERCA). 2-DG and IAA reduced the rate of reuptake of Ca^{2+} into the SR which was accompanied by a 15–20% decrease of SR Ca^{2+} load. Major changes of mitochondrial redox state (measured as FAD autofluorescence) were not observed after inhibition of glycolysis. Pyruvate (10 mM) and L-lactate (10 mM) elicited similar changes of the $[Ca^{2+}]_i$ transient. Pyruvate, L-lactate and IAA – but not 2-DG – induced intracellular acidosis. Recording of single channel activity of ryanodine receptors (RyRs) incorporated into lipid bilayers revealed complex modulation by glycolytic intermediates and products (1 mM each): some were without effect (G6P, PEP, L-lactate) while others either increased (F6P, +40%; FBP, +265%) or decreased (pyruvate, −58%) the open probability of the RyR. Consistent with these findings, spontaneous SR Ca^{2+} release (Ca^{2+} sparks) in permeabilized myocytes was facilitated by FBP and inhibited by pyruvate. The results indicate that in atrial myocytes glycolysis regulates Ca^{2+} release from the SR by multiple mechanisms including direct modulation of RyR activity by intermediates and products of glycolysis and modulation of SERCA activity through local changes of glycolytically derived ATP.

(Resubmitted 5 November 2004; accepted after revision 28 January 2005; first published online 3 February 2005)
Corresponding author L. A. Blatter, Department of Physiology, Stritch School of Medicine, Loyola University Chicago, 2160 South First Avenue, Maywood, IL 60153, USA. Email: lblatte@lumc.edu

Glycolysis, the metabolic pathway that converts glucose to the monocarboxylates pyruvate or L-lactate, is highly regulated by multiple factors (Opie, 1995). The most important enzymes for the regulation of glycolytic flux are phosphofructokinase (PFK) and glyceraldehyde 3-phosphate dehydrogenase (GAPDH). PFK activity is stimulated by a decrease of [ATP] and [creatine phosphate] ([CP]) and an increase of [inorganic phosphate] ($[P_i]$). Conversely, increases of [ATP] and [citrate] inhibit PFK activity. Thus, during normoxia, when cellular [ATP] and [citrate] are high, the rate of glycolysis is low. During ischaemia, however, when oxidative phosphorylation ceases and global [ATP], [CP], and [citrate] decline, glycolysis becomes accelerated severalfold. L-Lactate is produced in large amounts reaching concentrations exceeding 30 mM (Allen *et al.* 1989) and intracellular pH decreases to values < 6.5 (Allen *et al.* 1989; Elliott *et al.* 1992). Furthermore, cytosolic [NADH] increases because of the diminished rate of oxidative phosphorylation in the mitochondria. Elevated concentrations of cytosolic L-lactate, protons and NADH combine to inhibit GAPDH resulting in a strong inhibition of glycolytic flux during severe ischaemia.

In the normally oxygenated heart, the amount of glycolytically generated ATP is negligible compared to the amount produced by oxidative phosphorylation in the mitochondria. Nonetheless, aerobic glycolysis

J. Kockskämper and A. V. Zima contributed equally to this work.

DOI: 10.1113/jphysiol.2004.078782

has been shown to be critical for normal cardiac excitation–contraction (E–C) coupling. Inhibition of aerobic glycolysis may cause Ca^{2+} alternans and/or depression of excitability and $[Ca^{2+}]_i$ transients in cardiac myocytes (O'Rourke *et al.* 1994; Hüser *et al.* 2000; Kockskämper & Blatter, 2002). The tight functional coupling between glycolysis and E–C coupling is thought to be due to a close association of glycolytic enzymes and ion channels, transporters, and pumps participating in the E–C coupling process (Han *et al.* 1992; Xu *et al.* 1995). Accordingly, a number of membrane transport systems are regulated preferentially by glycolytically derived ATP including the sarcolemmal K_{ATP} channel (Weiss & Lamp, 1987, 1989), voltage-gated Ca^{2+} channels (Losito *et al.* 1998), the Na^+–K^+ pump (Glitsch & Tappe, 1993), the Na^+–H^+ exchanger (Wu & Vaughan-Jones, 1994; Sugiyama *et al.* 2001), and the sarcoplasmic reticulum (SR) Ca^{2+} pump (Xu *et al.* 1995). Furthermore, some studies also revealed that ion channels involved in E–C coupling may be modulated directly by intermediates of the glycolytic pathway. For example, the ryanodine receptor (RyR), the Ca^{2+} release channel of the SR, was found to be stimulated by glucose and fructose phosphates (Kermode *et al.* 1998). In addition, it was suggested that the activity of the sarcolemmal Na^+ channel is modulated directly by 2,3-bisphosphoglycerate and glyceraldehyde phosphate (Kohlhardt *et al.* 1989), although later experiments found no evidence for a direct modulation of Na^+ channel activity by inhibition of glycolysis (Mejia-Alvarez & Marban, 1992).

The aim of the present work was to gain detailed insight into the regulatory effects of glycolysis on atrial E–C coupling. In particular, we sought to identify the molecular mechanisms underlying the modulation of SR Ca^{2+} release by glycolysis. The results revealed that glycolytic intermediates and products exert distinct stimulatory and inhibitory effects on RyR-mediated SR Ca^{2+} release. In addition, glycolytically derived ATP was found to be important for the modulation of SR Ca^{2+} release as well as Ca^{2+} uptake. Acidosis, as occurs during ischaemia, and reduction of SR Ca^{2+} content were not a prerequisite for but may certainly contribute to this complex regulation of SR Ca^{2+} release by glycolysis.

Methods

Isolation of cat atrial myocytes

Single myocytes from the cat left atrium were isolated as previously described (Wu *et al.* 1991). The procedure for cell isolation was fully approved by the Institutional Animal Care and Use Committee of Loyola University Medical Center. Briefly, cats were anaesthetized with thiopental sodium (35 mg kg^{-1}, I.P.). After thoracotomy, hearts were excised, mounted on a Langendorff apparatus, and retrogradely perfused via the aorta with oxygenated collagenase-containing solution (37°C). Cells were plated on glass coverslips and 45–60 min were allowed for adherence. All experiments were performed at room temperature (22–25°C).

Ca^{2+} imaging

For Ca^{2+} imaging atrial myocytes were loaded with fluo-4 (Molecular Probes, Eugene, OR, USA) by 30–40 min exposure to Tyrode solution (mM: 140 NaCl, 5 KCl, 2 $CaCl_2$, 1 $MgCl_2$, 10 glucose, and 10 Hepes; pH 7.4 with NaOH) containing 20–45 μM of the acetoxymethylester of the Ca^{2+} indicator. A coverslip with dye-loaded myocytes was transferred to the stage of an inverted microscope (Nikon) equipped with a × 60 1.2 NA water immersion or a × 40 1.3 NA oil immersion objective lens. Cells were continuously superfused with Tyrode solution and stimulated at constant frequency (0.5–0.7 Hz) via a pair of extracellular platinum electrodes. Fifteen to twenty minutes was allowed for de-esterification of the indicator. Two-dimensional, confocal Ca^{2+} imaging was performed using a Nipkow dual-disc laser scanning unit (CSU10, Yokogawa Electric Co., Tokyo, Japan) and an intensified CCD camera (Stanford Photonics, Palo Alto, CA, USA), essentially as described before (Kockskämper *et al.* 2001). In addition, some experiments were carried out using the linescan mode of a Bio-Rad Radiance 2000 MP confocal imaging system (Bio-Rad, UK) as previously described (Zima *et al.* 2003*b*). In these experiments, the scan line was positioned at a central axial depth parallel to the longitudinal axis of the myocyte avoiding the nucleus. Temporal and spatial resolutions were 30 Hz and 0.3 μm × 0.3 μm for two-dimensional imaging and 166–333 Hz and 0.2 μm for linescan imaging. Fluo-4 was excited by the 488 nm line of an argon ion laser and emitted fluorescence was collected at wavelengths > 515 nm. Changes of $[Ca^{2+}]_i$ are expressed as changes of background-corrected normalized fluorescence (F/F_0), where F is the fluorescence intensity and F_0 is resting fluorescence recorded under steady-state conditions at the beginning of an experiment.

The cell surface membrane of atrial myocytes was permeabilized by adding 0.005% saponin as described before (Zima *et al.* 2003*b*). Ca^{2+} spark frequency was determined as number of observed sparks per second and per 100 μm of scanned distance in the confocal linescan mode (sparks s^{-1} (100 μm)$^{-1}$) and normalized to the frequency encountered under control conditions (see Fig. 10). The internal solution was composed of (mM): potassium aspartate 100; KCl 15; KH_2PO_4 5; MgATP 5; EGTA 0.4; $CaCl_2$ 0.12; $MgCl_2$ 0.75; phosphocreatine 10; creatine phosphokinase 5 U ml^{-1}; dextran (molecular mass 40 000) 8%; Hepes 10; fluo-3 potassium salt 0.04; pH 7.2 (KOH). Free $[Ca^{2+}]$ and $[Mg^{2+}]$ of this solution were 100 nM and 1 mM, respectively.

Alternans of the $[Ca^{2+}]_i$ transient amplitude (Ca^{2+} alternans) was quantified as the alternans ratio (AR) defined as $AR = 1 - S/L$, where S and L are the amplitudes of the small and large $[Ca^{2+}]_i$ transients, respectively (Kockskämper & Blatter, 2002). Thus, the AR can have values between 1 and 0. An AR of 0 indicates no alternans, whereas an AR of 1 indicates the highest possible degree of alternans with only every other stimulation resulting in a detectable $[Ca^{2+}]_i$ transient. Ca^{2+} alternans was defined as an AR exceeding 0.10.

SR Ca^{2+} load measurements

The amplitude of the $[Ca^{2+}]_i$ transient elicited by rapid exposure to 10 mM caffeine served as a measure of SR Ca^{2+} load. In order to determine whether the large caffeine-induced $[Ca^{2+}]_i$ signals could potentially saturate the indicator and distort the SR Ca^{2+} load estimates, we conducted *in vivo* measurements of F_{max}, i.e. measurements of fluo-4 fluorescence under Ca^{2+}-saturating conditions. F_{max} was determined *in vivo* by exposure of fluo-4-loaded myocytes to the detergent saponin (0.01%) in the presence of 2 mM extracellular Ca^{2+}. In these experiments the average caffeine-induced $[Ca^{2+}]_i$ transient amplitude amounted to only 64% of F_{max} ($n = 4$). Thus, we concluded that during caffeine exposure the intracellular Ca^{2+} indicator was not saturated.

Measurements of flavoprotein-linked autofluorescence

Flavin adenine dinucleotide (FAD)-linked mitochondrial autofluorescence, a direct indicator of mitochondrial redox state, was measured by means of laser scanning confocal microscopy (Bio-Rad Radiance 2000 MP, Bio-Rad, UK) as previously described (Romashko *et al.* 1998; Zima *et al.* 2003*b*). FAD-linked autofluorescence of isolated myocytes was excited at 488 nm and fluorescence was collected at wavelengths > 515 nm. Two-dimensional images were acquired at 15 s intervals. After background subtraction, relative changes of autofluorescence (F/F_0) integrated over regions of interest (approximately 10 μm × 10 μm) are reported.

Measurements of intracellular pH

Intracellular pH (pH_i) was measured using laser scanning confocal microscopy as previously described (Zima *et al.* 2003*b*). Cells were loaded with the pH indicator 5-(and-6)-carboxy SNARF-1 (Molecular Probes) by 30–40 min exposure to Tyrode solution containing 9 μM of the acetoxymethylester acetate of the dye. SNARF-1 was excited at 514 nm, and emitted fluorescence was collected simultaneously at 590 ± 35 nm (F_{590}) and at > 650 nm ($F_{>650}$). Data were recorded at 15–60 s intervals. After background correction, the ratio $F_{>650}/F_{590}$ was used as an index of pH with higher values indicating alkalinization and lower values indicating acidification. Changes of pH (ΔpH) were calculated by averaging five data points immediately preceding and following application of a test substance. The difference was taken as ΔpH and normalized to an initial application of 10 mM pyruvate (see Fig. 7).

Ryanodine receptor single channel recordings

Single channel activity of isolated ryanodine receptors (RyRs) incorporated into planar lipid bilayers was measured as previously described (Zima *et al.* 2003*b*). Briefly, RyR-containing SR vesicles obtained from rat ventricles were fused with bilayers formed from a lipid mixture of phosphatidylethanolamine, phosphatidylserine, and phosphatidylcholine (ratio 5 : 4 : 1) dissolved in *n*-decane at a final lipid concentration of 45 mg ml^{-1}. For recording of Cs^+ currents through RyRs, the *cis*- and *trans*-chambers contained (mM): $CsCH_3SO_3$ 400; $CaCl_2$ 0.1; Hepes 20; pH 7.3. Free $[Ca^{2+}]$ in the (cytosolic) *cis*-chamber was adjusted to 3 μM with EGTA. Single channel currents were recorded with an Axopatch 200B amplifier (Axon Instruments, Union City, CA, USA) at a holding potential of −20 mV. Currents were filtered at 1 kHz and sampled at 5 kHz.

Drugs

Glucose-6-phosphate (G6P), fructose-6-phosphate (F6P), fructose-1,6-bisphosphate (FBP), phosphoenolpyruvate (PEP), pyruvate, L-lactate, D-lactate, 2-deoxy-D-glucose (2-DG), iodoacetic acid (IAA), and cyanide (CN^-) were purchased from Sigma-Aldrich and directly dissolved in the experimental solutions at concentrations as indicated in the text. G6P and PEP were purchased as mono-potassium salts, F6P and FBP as di-potassium salts, and pyruvate, lactate IAA and CN^- as mono-sodium salts. In experiments where pyruvate- and lactate-containing Tyrode solutions were used NaCl in control Tyrode solution was increased by an equimolar amount to keep $[Na^+]_o$ constant throughout the experiment and to avoid solution-induced changes in the activity of Na^+–Ca^+ exchange. Carbonyl cyanide *p*-trifluoromethoxy-phenylhydrazone (FCCP) was prepared as stock solution in methanol and diluted in the extracellular solution to yield the desired concentrations.

Data analysis

Data are presented as means ± standard error of the mean (S.E.M.) of *n* measurements. Statistical comparisons between groups were performed with Student's *t* test. A difference statistically not significant at $P = 0.05$ is indicated by 'N.S.'.

Results

Inhibitors of glycolysis impair E–C coupling in atrial myocytes

In cardiac myocytes, glycolysis and excitation–contraction coupling appear to be tightly coupled (O'Rourke *et al.* 1994; Hüser *et al.* 2000). Figure 1 compares the effects of substrate-free Tyrode solution (SF, omission of glucose) and two inhibitors of glycolysis, 2-deoxy-D-glucose (2-DG, 10 mM) and iodoacetate (IAA, 1 mM), on action potential (AP)-induced $[Ca^{2+}]_i$ transients in isolated cat atrial myocytes. Exposure of a cell to substrate-free solution caused a slight decrease of the amplitude of the $[Ca^{2+}]_i$ transient (Fig. 1*A*, top panel). After 6 min in glucose-free Tyrode solution $[Ca^{2+}]_i$ transient amplitude amounted to $96 \pm 5\%$ ($n = 5$; N.S.) of control. By contrast, inhibition of glycolysis by either 2-DG or IAA exerted profound effects on Ca^{2+} homeostasis (Fig. 1*A*, middle and bottom panels). Typically, 2-DG or IAA caused Ca^{2+} alternans and a decrease in the amplitude of the $[Ca^{2+}]_i$ transient. Ca^{2+} alternans occurred after about 2–4 min. Average ARs amounted to 0.34 ± 0.06 ($n = 19$; $P < 0.001$) for 2-DG and 0.28 ± 0.05 ($n = 21$; $P < 0.01$) for IAA (Fig. 1*B*). In addition, a decrease in $[Ca^{2+}]_i$ transient amplitude was observed. $[Ca^{2+}]_i$ transient amplitude decreased to $50 \pm 6\%$ ($n = 19$; $P < 0.001$) and to $62 \pm 5\%$ ($n = 21$; $P < 0.001$) after 6 min of 2-DG or IAA application, respectively. It should be noted that the degree of glycolysis-mediated alterations

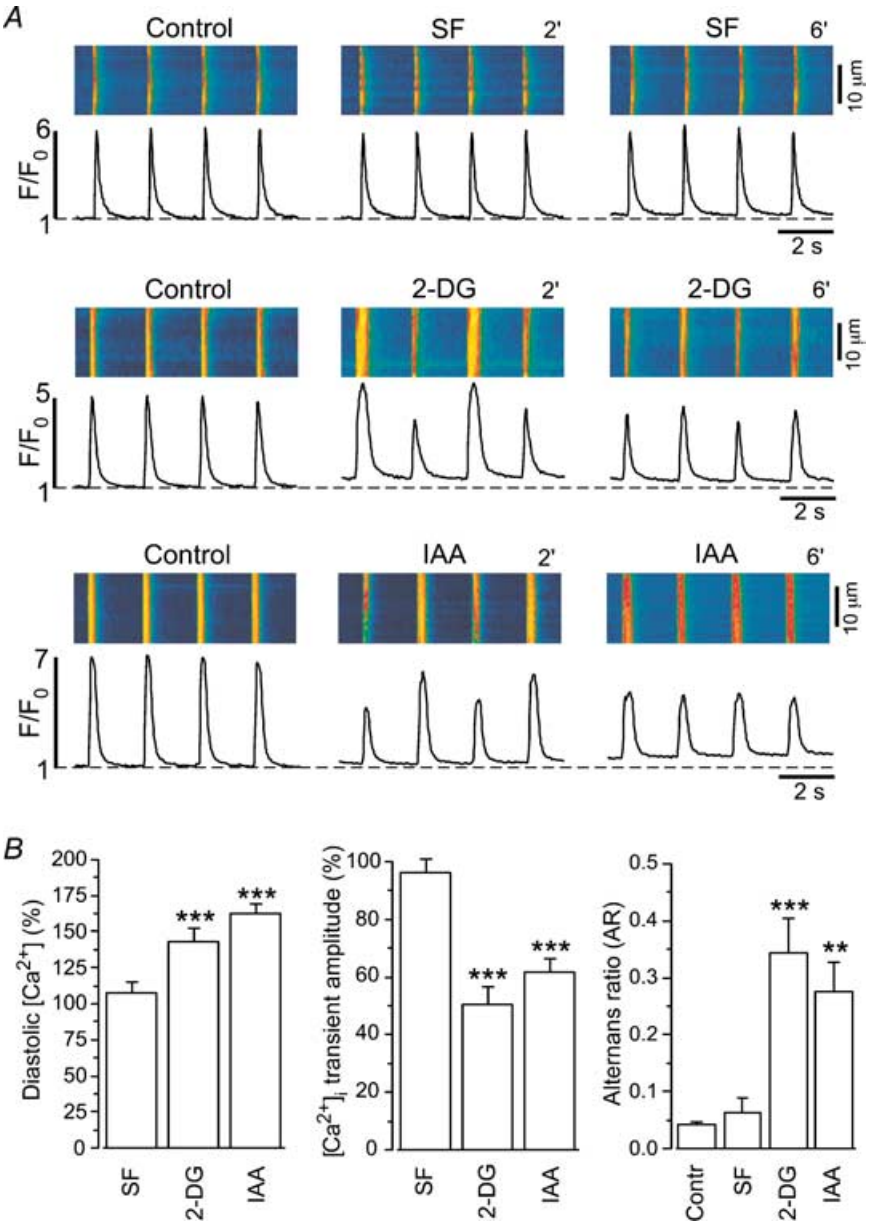

Figure 1. Effects of glycolytic inhibitors on electrically evoked $[Ca^{2+}]_i$ transients in atrial myocytes
A, confocal linescan images (fluo-4 fluorescence) and corresponding F/F_0 plots recorded from three atrial myocytes. Substrate-free (SF) solution (top panel) did not affect the $[Ca^{2+}]_i$ transient. By contrast, both 2-deoxy-D-glucose (2-DG, 10 mM; middle panel) and iodoacetic acid (IAA, 1 mM; bottom panel) increased diastolic $[Ca^{2+}]_i$, induced Ca^{2+} alternans and decreased the amplitude of the $[Ca^{2+}]_i$ transient. 2′, 2 min; 6′, 6 min. *B,* mean values obtained from five (SF), 19 (2-DG), and 21 (IAA) atrial myocytes. Average diastolic $[Ca^{2+}]_i$ and amplitudes were measured 6 min after exposure to the test solutions and normalized to control conditions. AR was calculated when Ca^{2+} alternans was pronounced. In the case of alternans the average amplitude was calculated from four consecutive $[Ca^{2+}]_i$ transients, i.e. from 2 pairs of a small and a large transient. $^{**}P < 0.01$; $^{***}P < 0.001$.

of the $[Ca^{2+}]_i$ transient varied significantly from cell to cell, ranging from almost complete inhibition (see Figs 2*A*, 6 min (6′)) to steady-state Ca^{2+} alternans (Figs 1 and 2*B*). Furthermore, inhibition of glycolysis by 2-DG or IAA increased diastolic $[Ca^{2+}]_i$ by $43 \pm 9\%$ ($n = 19$; $P < 0.001$) and $62 \pm 7\%$ ($n = 21$; $P < 0.001$), respectively (Fig. 1*B*), whereas substrate-free conditions had no significant effect on diastolic $[Ca^{2+}]_i$. Thus, withdrawal of glucose alone was not sufficient to depress $[Ca^{2+}]_i$ transients. Block of glycolytic enzymes, however, elicited rapid and significant suppression of AP-induced $[Ca^{2+}]_i$ transients suggesting that an intact glycolytic pathway is necessary to maintain E–C coupling in these cells.

The inhibitory effects of 2-DG and IAA on atrial $[Ca^{2+}]_i$ transients were concentration dependent. At 2 mM, 2-DG caused a decrease of $[Ca^{2+}]_i$ transient amplitude to $79 \pm 3\%$ of control and an increase of diastolic $[Ca^{2+}]_i$ by $24 \pm 10\%$ ($n = 4$). Similarly, low concentrations of IAA (0.2–0.5 mM) elicited moderate decreases of $[Ca^{2+}]_i$ transient amplitude and increases of diastolic $[Ca^{2+}]_i$. However, both compounds at these lower concentrations did not induce significant Ca^{2+} alternans (data not shown).

The observed changes in $[Ca^{2+}]_i$ transient amplitude during inhibition of glycolysis could be the result of a decrease in SR Ca^{2+} content. Therefore, we determined SR Ca^{2+} load during inhibition of glycolysis by either 2-DG or IAA using rapid caffeine applications. Figure 2*A* and *B* shows representative experiments from two different atrial myocytes in which 10 mM caffeine was applied under control conditions and after 2 and 6 min of exposure to either 2-DG (Fig. 2*A*) or IAA (Fig. 2*B*), respectively. In both cases, caffeine-releasable SR Ca^{2+} declined during inhibition of glycolysis. On average, the amplitude of the caffeine response in the presence of 2-DG or IAA was reduced to $83 \pm 3\%$ ($n = 12$; $P < 0.001$) and $82 \pm 3\%$ ($n = 10$; $P < 0.001$) of control, respectively (Fig. 2*C*). Furthermore, the decay kinetics of the $[Ca^{2+}]_i$ transients were slowed in the presence of 2-DG and IAA (Fig. 3*A* and *B*; Table 1), suggesting that Ca^{2+} removal either by the SERCA and/or via Na^+–Ca^+ exchange (NCX) might be affected by inhibition of glycolysis.

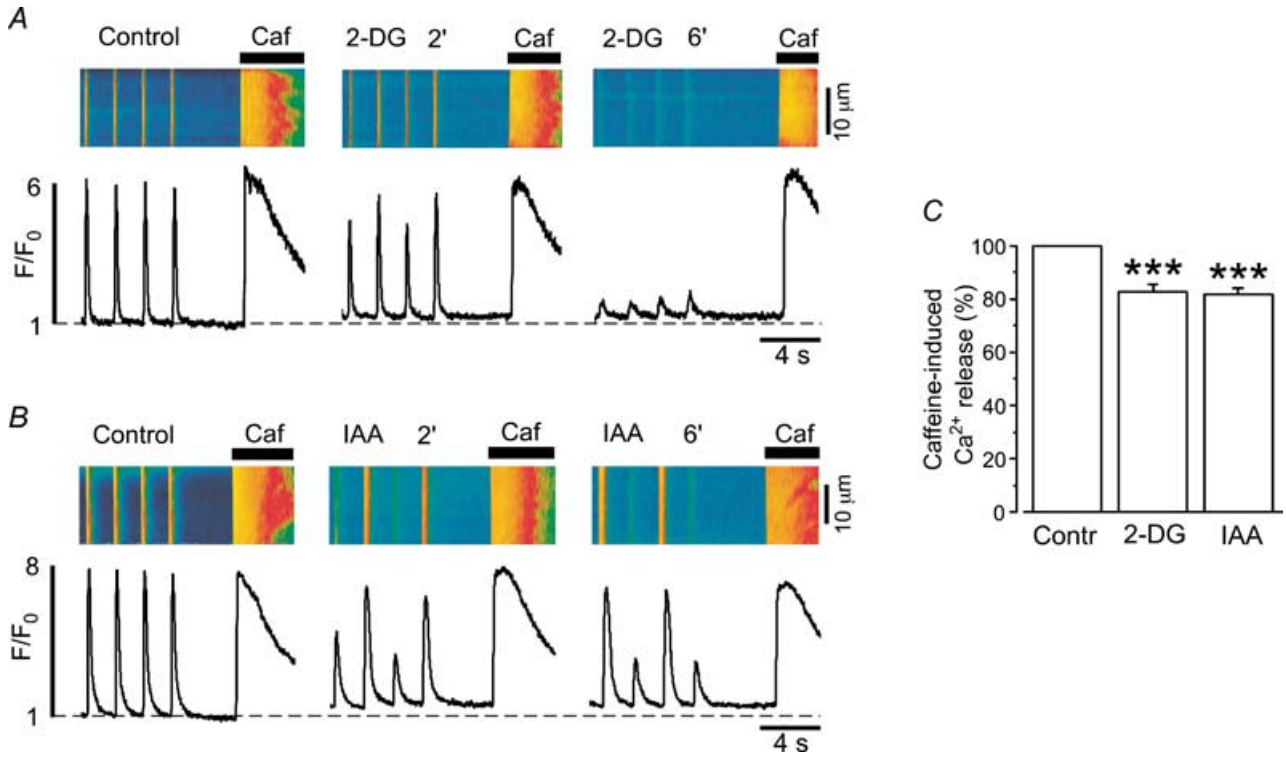

Figure 2. Sarcoplasmic reticulum Ca^{2+} load during inhibition of glycolysis in intact atrial myocytes
A and *B*, confocal linescan images (fluo-4 fluorescence) and corresponding F/F_0 plots of $[Ca^{2+}]_i$ transients and caffeine (10 mM)-releasable SR Ca^{2+} content in two atrial myocytes before and during inhibition of glycolysis by 2-DG (10 mM, *A*) or IAA (1 mM, *B*). Recordings were made 2 and 6 min after application of 2-DG or IAA had started. *C*, average values of caffeine-releasable SR Ca^{2+} content 6 min after exposure of the cells to either 2-DG or IAA. Values are normalized to the amplitude of caffeine-induced Ca^{2+} release before application of 2-DG ($n = 12$) or IAA ($n = 10$). During Ca^{2+} alternans SR Ca^{2+} load was not significantly different whether it was measured after a small or a large amplitude $[Ca^{2+}]_i$ transient (see also Hüser *et al.* 2000). ***$P < 0.001$.

Effects of 2-DG and IAA on Ca^{2+} removal

We gained further insight into the relative contributions of SERCA and NCX to Ca^{2+} removal from a quantitative kinetic analysis of $[Ca^{2+}]_i$ decline during twitch- and caffeine-induced $[Ca^{2+}]_i$ transients. The analysis is based on the notion that the decline of $[Ca^{2+}]_i$ during the caffeine-induced $[Ca^{2+}]_i$ transient (in the maintained presence of caffeine) is due to NCX, whereas during the AP-induced (twitch) $[Ca^{2+}]_i$ transient $[Ca^{2+}]_i$ declines as the result of the combined activities of SERCA and NCX. (Slow Ca^{2+} transport by mitochondria and sarcolemmal Ca^{2+} ATPase is considered to be small, accounting in most species, including cats, to only 1–2% of total Ca^{2+} transport; see Bers, 2001.) Figure 3*A* and *B* shows that 2-DG and IAA slowed the decline of the twitch $[Ca^{2+}]_i$ transient, but did not affect the kinetics of the caffeine-induced $[Ca^{2+}]_i$ transient. Table 1 shows that the rate of decline of twitch $[Ca^{2+}]_i$ (derived from a mono-exponential fit to the $[Ca^{2+}]_i$ transient) was significantly slowed (no. 1 in Table 1). Both inhibitors, 2-DG and IAA, decreased the rate constant by approximately 30% (Table 1), suggesting that the glycolytic inhibitors primarily affected the activity of SERCA (no. 3 in Table 1), but not NCX (no. 2 in Table 1).

The decay kinetics of $[Ca^{2+}]_i$ transients were analysed further to derive V_{max} and K_m (for definitions see footnote to Table 1) and to estimate the relative contributions of

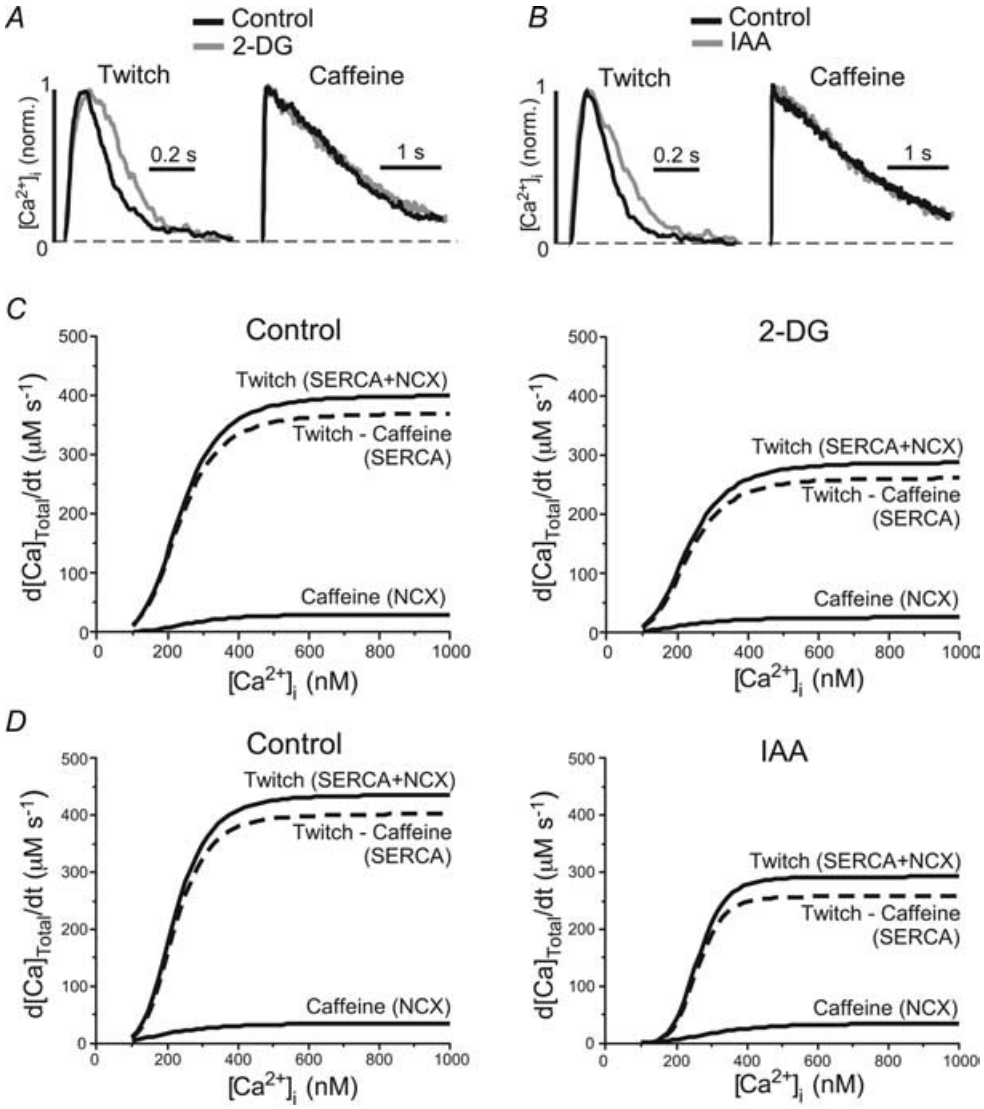

Figure 3. $[Ca^{2+}]_i$ dependence of Ca^{2+} removal fluxes during inhibition of glycolysis
A and *B*, normalized twitch- and caffeine-induced $[Ca^{2+}]_i$ transients under control conditions (black traces) and in the presence of the glycolytic inhibitors (grey traces) 2-DG (panel *A*) and IAA (panel *B*). *C*, Ca^{2+} transport functions derived from twitch and caffeine-induced $[Ca^{2+}]_i$ transients under control conditions (left) and in the presence of 2-DG. For details of the method see text and legend of Table 1. *D*, same analysis as in panel *C*, but for IAA.

Table 1. Rate of decline of $[Ca^{2+}]_i$ transients evoked by electrical stimulation (twitch) or by fast caffeine application and kinetic parameters of Ca^{2+} transport systems

		Control ($n = 22$)	2-DG ($n = 12$)	IAA ($n = 10$)
1	Rate of $[Ca^{2+}]_i$ decline (s^{-1}); twitch (SERCA + NCX)	10.9 ± 0.7	7.8 ± 0.6**	7.9 ± 0.6*
2	Rate of $[Ca^{2+}]_i$ decline (s^{-1}); caffeine (NCX)	0.63 ± 0.05	0.59 ± 0.04	0.57 ± 0.04
3	(1) – (2) (s^{-1}); (SERCA)	10.2 ± 0.7	7.2 ± 0.6**	7.3 ± 0.6*
4	V_{max} ($\mu M\ s^{-1}$); total Ca^{2+} removal (SERCA + NCX)	513 ± 35	366 ± 33**	336 ± 47**
5	V_{max} ($\mu M\ s^{-1}$); (NCX)	23 ± 1	22 ± 1	20 ± 1
6	V_{max} ($\mu M\ s^{-1}$); (SERCA)	493 ± 35	345 ± 33**	318 ± 46**
7	K_m (nM); total Ca^{2+} removal (SERCA + NCX)	231 ± 6	222 ± 8	298 ± 28*
8	K_m (nM); (NCX)	374 ± 30	351 ± 38	375 ± 37
9	K_m (nM); (SERCA)	232 ± 6	221 ± 9	295 ± 28*

The rate of $[Ca^{2+}]_i$ decline was derived from a mono-exponential fit to the decaying phase of the $[Ca^{2+}]_i$ transient. Ca^{2+} transport parameters were calculated by the method developed by Bassani *et al.* (1994). $[Ca^{2+}]_i$ was calculated from F/F_0 according to Hüser *et al.* (2000) and $[Ca^{2+}]_i$ was converted to total cytosolic $[Ca^{2+}]$ ($[Ca^{2+}]_{Total}$) using buffering data from Bers (2001):

$$[Ca]_{Total} = \{236\,\mu M/(1 + (498\,nM/[Ca^{2+}]_i))\} - 39\,\mu M.$$

$d[Ca^{2+}]_{Total}/dt$ is plotted as a function of $[Ca^{2+}]_i$ for each point of time during $[Ca^{2+}]_i$ decline. The data were then fitted by a Hill equation:

$$V = V_{max}/\{1 + (K_m/[Ca^{2+}]_i)^n\},$$

to determine the parameters V_{max} (maximum velocity), K_m (Michaelis–Menten constant) and n (Hill coefficient). *Statistically significant at $P < 0.05$; **statistically significant at $P < 0.01$.

SERCA and NCX, using the method developed by Bassani *et al.* (1994). First, we plotted the total (SERCA + NCX) Ca^{2+} removal flux and the NCX flux ($d[Ca^{2+}]_{Total}/dt$) obtained from twitch and caffeine-induced $[Ca^{2+}]_i$ transients, respectively, as a function of $[Ca^{2+}]_i$ (Fig. 3*C* and *D*, continuous curves). The data revealed that in atrial myocytes overall the contribution from NCX is relatively small (less then 8%) compared to SERCA (Fig. 3*C* and *D*, and Table 1). Then the Ca^{2+} flux attributable to NCX was subtracted from the total Ca^{2+} removal flux to derive the contribution of SERCA (Fig. 3*C* and *D*; dashed curves). V_{max} and K_m of all transport fluxes are summarized in Table 1. The analysis revealed that 2-DG and IAA decreased V_{max} of SERCA (measured after 6 min of exposure to the inhibitors) by 30% ($n = 12$; $P < 0.01$) or by 35% ($n = 10$; $P < 0.01$), respectively. In contrast, 2-DG and IAA did not change V_{max} of NCX. Thus, the analysis revealed that 2-DG and IAA had a profound inhibitory effect on SERCA.

We also tested the effect of glycolytic inhibitors on SERCA activity with a different experimental approach. We compared the recovery of twitch $[Ca^{2+}]_i$ transients after complete depletion of the SR in the presence and absence of glycolytic inhibitors. Individual atrial myocytes were exposed to 10 mM caffeine to completely deplete the SR (Fig. 4*A*). After recovery of the caffeine-induced $[Ca^{2+}]_i$ transient and removal of caffeine from the bath solution electrical stimulation resumed. The electrically evoked $[Ca^{2+}]_i$ transients revealed a positive staircase phenomenon and the $[Ca^{2+}]_i$ transient amplitude fully recovered over the course of 10–12 twitches (Fig. 4*B*). After 6 min of exposure to 2-DG, recovery of the $[Ca^{2+}]_i$ transient after SR depletion was slowed significantly. On average $t_{1/2}$ of $[Ca^{2+}]_i$ transient amplitude recovery (i.e. the time elapsed between the first twitch after store depletion and recovery of twitch amplitude to 50% of control) increased from 8.1 ± 1.4 s to 14.8 ± 1.6 s ($n = 5, P < 0.05$). Similar observations were made with IAA (Fig. 4*C* and *D*). IAA increased $t_{1/2}$ from 8.4 ± 1.0 s to 13.9 ± 0.7 s ($n = 6$, $P < 0.05$).

Thus, a reduced SERCA activity during inhibition of the glycolytic pathway contributes to a decrease in SR Ca^{2+} load (Fig. 2*C*), which, in turn, can decrease (or alter) SR Ca^{2+} release. It should be noted, however, that in some cases typical glycolysis-dependent alterations of the $[Ca^{2+}]_i$ transient occurred when SR Ca^{2+} load was almost identical to control (e.g. Fig. 2*A*, compare first and third caffeine application). This finding indicates that the inhibitory effects of 2-DG and IAA on atrial $[Ca^{2+}]_i$ transients cannot be explained entirely by reduced SR Ca^{2+} content. The data suggest that other mechanisms must exist that contribute to the observed alterations of the $[Ca^{2+}]_i$ transient.

Effects of 2-DG and IAA on mitochondrial redox state

Since glycolytic products are essential fuels for respiratory ATP production, block of glycolysis by IAA or 2-DG might have affected the metabolic state of the cells. Thus, we investigated whether the observed effects of 2-DG and IAA on atrial E–C coupling were the result of inhibition of mitochondrial respiration with subsequent decrease in ATP levels. To this end, we measured the effects of 2-DG and IAA on FAD-linked mitochondrial autofluorescence in intact atrial myocytes. Figure 5 illustrates the experimental protocol and average results. First, cells were challenged with 2-DG (10 mM, Fig. 5*A*) or IAA (1 mM, Fig. 5*B*) to find out whether the respective treatment leads to changes in FAD-linked autofluorescence. Then, CN^- (4 mM) and FCCP (1 μM) were applied to induce maximum reduction and oxidation, respectively, of the mitochondrial FAD/$FADH_2$ system. At the beginning of the experiments, mitochondria were in an almost fully reduced state (~80% of the normalized FCCP-CN^- signal). Application of both 2-DG and IAA slightly increased the FAD signal (F/F_0) to 1.07 ± 0.02 (2-DG, $n = 7$; $P < 0.05$) and 1.03 ± 0.01 (IAA, $n = 33$, $P < 0.05$), respectively. Exposure of the cells to CN^- decreased FAD fluorescence to 0.78 ± 0.01 ($n = 40$; $P < 0.001$), whereas FCCP increased it to 2.06 ± 0.04 ($n = 40$; $P < 0.001$). Thus, the changes induced by inhibition of glycolysis accounted for a reduction of mitochondrial redox state of less than 5%. While these small changes were statistically significant ($P < 0.05$) they had no effect on AP- and caffeine-induced $[Ca^{2+}]_i$ transients. We found that exposure to 10 nM FCCP caused approximately the same changes in FAD signal as 2-DG and IAA; however, in the presence of 10 nM FCCP, twitch $[Ca^{2+}]_i$ transients and SR Ca^{2+} load were not different from control (data not shown). Therefore, we concluded that the small effect of 2-DG or IAA on mitochondrial redox state was highly unlikely to generate the observed effects on atrial E–C coupling through a generalized attenuation of cellular energy metabolism or depletion of cellular ATP reserves.

Glycolytic products impair E–C coupling in atrial myocytes

In a next step we studied the effects of the glycolytic products pyruvate and L-lactate on atrial $[Ca^{2+}]_i$ transients (Fig. 6). Both compounds can inhibit glycolysis (see Opie, 1995), L-lactate at the level of GAPDH and pyruvate at the level of PFK. Original recordings of $[Ca^{2+}]_i$ transients from single myocytes challenged with L-lactate (10 mM) or pyruvate (10 mM) are displayed in Fig. 6*A*. Pyruvate (Fig. 6*A*, top panel) elicited an increase in diastolic $[Ca^{2+}]_i$,

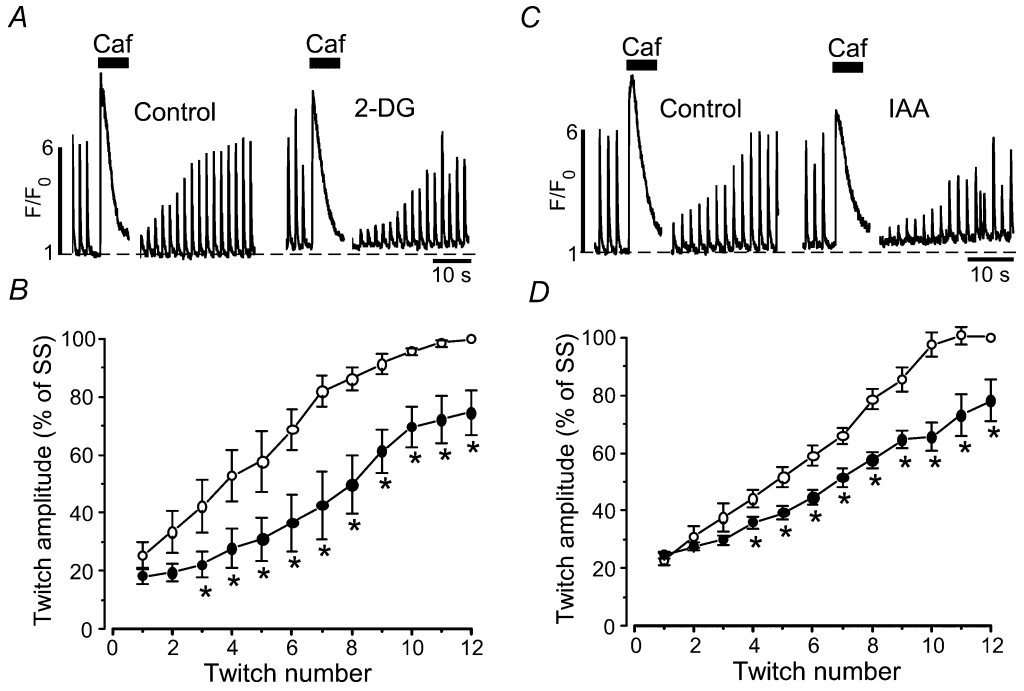

Figure 4. Effects of glycolytic inhibitors on recovery of $[Ca^{2+}]_i$ transients after SR depletion
A, electrically evoked $[Ca^{2+}]_i$ transients recorded before and after complete depletion of the SR with caffeine (10 mM) in normal Tyrode solution (Control) and in the presence of 2-DG (10 mM). Stimulation frequency 0.5 Hz. *B*, average normalized $[Ca^{2+}]_i$ transient amplitudes as a function of twitch number after SR depletion with caffeine in the presence of 2-DG ($n = 5$). The transients were normalized to the steady-state (SS) amplitude under control conditions (glucose-containing Tyrode solution) before exposure to caffeine. *C*, same experiment as in panel *A* but with IAA (1 mM). *D*, average normalized $[Ca^{2+}]_i$ transient amplitudes as a function of twitch number after SR depletion with caffeine in the presence of IAA ($n = 6$). $^*P < 0.05$.

a decrease of the $[Ca^{2+}]_i$ transient amplitude and Ca^{2+} alternans, as previously described (Hüser *et al.* 2000; Kockskämper & Blatter, 2002). L-Lactate caused similar alterations of the AP-induced $[Ca^{2+}]_i$ transient (Fig. 6*A*, bottom panel). Occasionally, spontaneous Ca^{2+} release (presumably due to spontaneous action potentials) was observed (marked by the filled circles in Fig. 6*A*, bottom panel). In addition, L-lactate decreased SR Ca^{2+} load on average by 14% ($n = 5$; $P = 0.001$), i.e. similar to 2-DG and IAA. On average, L-lactate and pyruvate increased diastolic $[Ca^{2+}]_i$ by $54 \pm 4\%$ ($n = 10$; $P < 0.001$) and $39 \pm 4\%$ ($n = 6$; $P < 0.05$), decreased $[Ca^{2+}]_i$ transient amplitude to $64 \pm 7\%$ ($n = 10$; $P < 0.01$) and $79 \pm 9\%$ ($n = 6$) and caused Ca^{2+} alternans with an AR of 0.36 ± 0.10 ($n = 10$; $P < 0.001$) and 0.34 ± 0.09 ($n = 6$; $P < 0.001$), respectively (Fig. 6*B*). D-Lactate caused alterations of the $[Ca^{2+}]_i$ transient that were almost identical to L-lactate ($n = 5$ cells; data not shown).

Pyruvate, lactate, and IAA, but not 2-DG, decrease intracellular pH

Acidosis has multiple effects on cardiac E–C coupling including the generation of alternans (Orchard *et al.* 1991; Diaz *et al.* 2002). Pyruvate, lactate and IAA are weak organic acids. Furthermore, pyruvate and lactate uptake by cardiac myocytes is mediated by a sarcolemmal monocarboxylate transporter that cotransports protons (Poole & Halestrap, 1993). Therefore, we considered the possibility that the observed effects of pyruvate, lactate, 2-DG, and IAA on atrial E–C coupling were caused by a decrease of intracellular pH (pH_i). Figure 7*A* shows pH changes in a cell challenged with pyruvate, L-lactate, and D-lactate. Each substance was applied for 5 min, and 6 min was allowed for washout. Pyruvate (10 mM) elicited a reversible decrease in the emission ratio of carboxy SNARF-1 fluorescence ($F_{>650}/F_{590}$) indicating acidification of the cytosol. L-Lactate and D-lactate caused acidifications of similar magnitude. Mean data from five atrial myocytes subjected to this protocol are shown in Fig. 7*C*. Changes of intracellular pH (ΔpH_i) were normalized to the initial acidification induced by pyruvate (100%). According to this comparison, decreases of pH_i mediated by L- and D-lactate amounted to $124 \pm 17\%$ ($n = 5$) and $120 \pm 21\%$ ($n = 5$), respectively. In a second set of experiments, cells were exposed to pyruvate, 2-DG, and IAA. An original recording from an atrial myocyte is illustrated in Fig. 7*B*. Again, pyruvate (10 mM) elicited a reversible acidification of the cytosol that served as an internal standard to evaluate the effect of the glycolytic inhibitors. IAA (1 mM) also decreased intracellular pH albeit to a smaller degree. Conversely, 2-DG (10 mM)

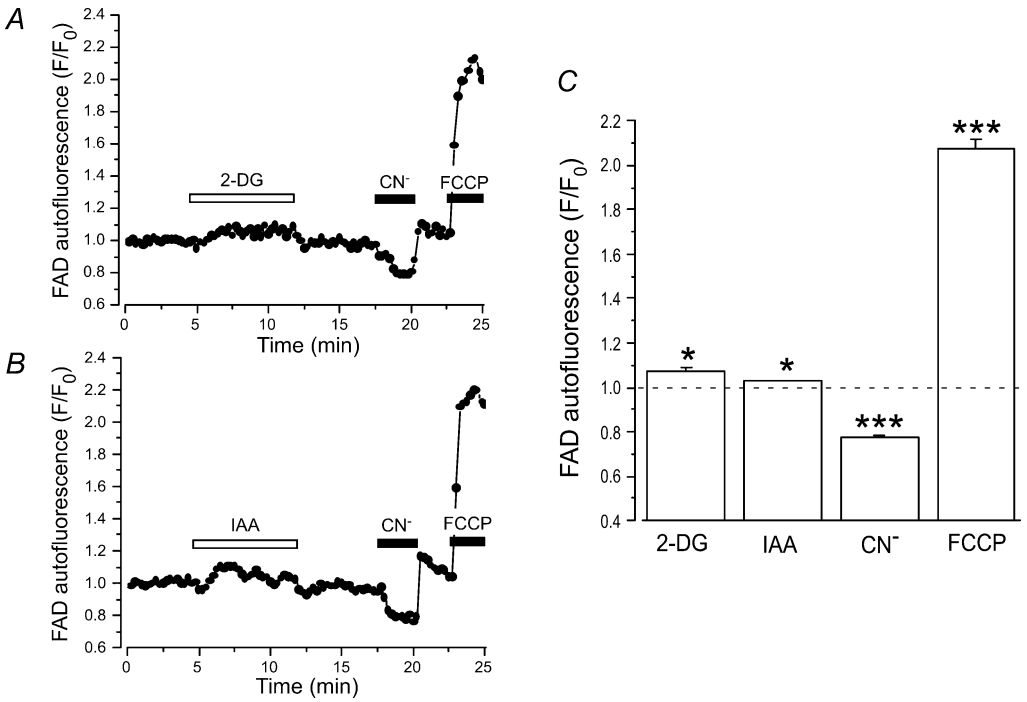

Figure 5. FAD-linked mitochondrial autofluorescence during inhibition of glycolysis
A and *B*, FAD-linked mitochondrial autofluorescence in two atrial myocytes challenged with 2-DG (10 mM, *A*) or IAA (1 mM, *B*). At the end of the experiments myocytes were treated with CN^- (4 mM) and FCCP (1 μM) to induce maximum reduction and oxidation, respectively, of the FAD/$FADH_2$ system. *C*, relative changes of FAD-linked autofluorescence during exposure of atrial myocytes to 2-DG ($n = 7$), IAA ($n = 33$), CN^- ($n = 40$), and FCCP ($n = 40$). $^*P < 0.05$; $^{***}P < 0.001$.

did not affect pH_i. Summarized data from seven cells confirmed these observations (Fig. 7*C*). In the presence of 2-DG, intracellular pH remained essentially unchanged ($0 \pm 4\%$, $n = 7$), whereas IAA caused an acidification that was on average half as large ($50 \pm 5\%$, $n = 7$) as the pyruvate-mediated acidification (100%). In conclusion, pyruvate, lactate and IAA reduced pH_i in cat atrial myocytes. Importantly, however, 2-DG did not change intracellular pH. Thus, it is concluded that the alterations of E–C coupling common to all four substances (i.e. increase of diastolic $[Ca^{2+}]_i$, decrease of $[Ca^{2+}]_i$ transient amplitude and generation of Ca^{2+} alternans) were not caused solely by acidification of the cytosol, but must involve additional mechanisms. These were further explored in the following experiments.

Focal application of 2-DG induces local Ca^{2+} alternans

Previous studies have revealed that cardiac Ca^{2+} alternans can be a local subcellular phenomenon (Kockskämper & Blatter, 2002; Diaz *et al.* 2004). Focal applications of IAA or pyruvate through a micropipette to part of an atrial myocyte resulted in Ca^{2+} alternans that was confined to the region of exposure. Distant regions upstream of the pipette tip were not affected and exhibited $[Ca^{2+}]_i$ transients of constant amplitude, leading us to suggest that atrial Ca^{2+} alternans may be generated, at least in part, by reduction of glycolytic flux in the microenvironment of RyRs, SR Ca^{2+} pumps, and/or sarcolemmal Na^+–Ca^+ exchangers (Kockskämper & Blatter, 2002). Since both IAA and pyruvate decrease pH_i it is possible that local Ca^{2+} alternans in previous experiments was caused by local acidification rather than local modulation of glycolytic flux. To distinguish between these possibilities, we tested whether local Ca^{2+} alternans could also be elicited by focal application of 2-DG, which inhibits glycolysis but, unlike IAA and pyruvate, did not change pH_i (see Fig. 7). Figure 8 illustrates such an experiment. The atrial myocyte and the position of the pipette tip are shown in Fig. 8*A*. The whole cell was continuously superfused with Tyrode solution (Bulk flow, arrows). Under these conditions, pressure ejection of the 2-DG-containing pipette solution ($[2\text{-DG}] = 5$ mM) resulted in spatially restricted application to only the right half of the myocyte (see also Kockskämper & Blatter, 2002). Local $[Ca^{2+}]_i$ transients of regions close to (*a*, proximal region) and distant from (*b*, distal region) the pipette tip were recorded before and after a focal application of 5 mM

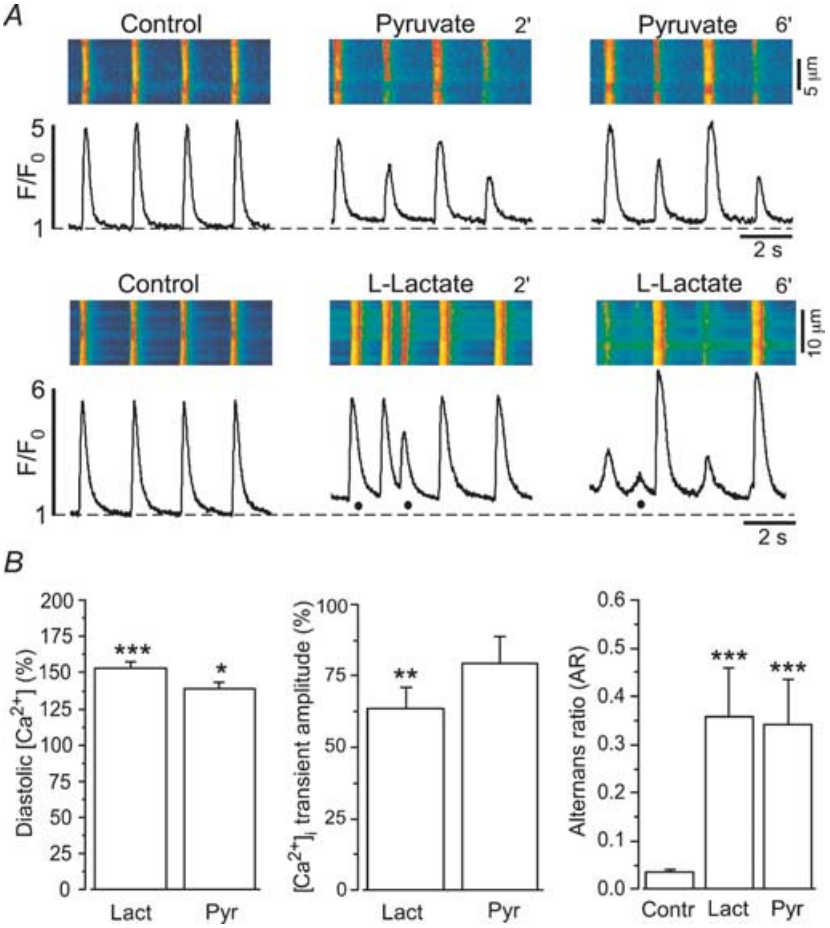

Figure 6. Effects of glycolytic products on electrically evoked $[Ca^{2+}]_i$ transients in atrial myocytes
A, confocal linescan images (fluo-4 fluorescence) and corresponding F/F_0 plots recorded from two atrial myocytes challenged with the glycolytic products pyruvate (10 mM, top) and L-lactate (10 mM, bottom). Changes of $[Ca^{2+}]_i$ transients induced by lactate and pyruvate resembled the changes mediated by inhibition of glycolysis (compare Fig. 1) including elevation of diastolic $[Ca^{2+}]_i$, induction of Ca^{2+} alternans, and decrease of the amplitude of the $[Ca^{2+}]_i$ transient. Filled circles mark spontaneous Ca^{2+} release events. *B,* mean values obtained from 10 (lactate, Lact) and 6 (pyruvate, Pyr) atrial myocytes. Average diastolic $[Ca^{2+}]_i$ and amplitudes were measured 6 min after exposure to the test solutions $^*P < 0.05$; $^{**}P < 0.01$; $^{***}P < 0.001$.

2-DG (Fig. 8*B*). Before exposure to the glycolytic inhibitor, both regions exhibited uniform $[Ca^{2+}]_i$ transients with similar amplitudes and no signs of Ca^{2+} alternans. Shortly after the 20 s application of 2-DG (box in Fig. 8*Ba*), the proximal region (*a*) displayed Ca^{2+} alternans (AR_a: 0.27) whereas the distal region (*b*) did not (AR_b: 0.04). Figure 8*C* compares the average ARs obtained from proximal (filled bar) and distal (open bar) regions in a total of four atrial myocytes. Ca^{2+} alternans was only observed at regions close to the pipette tip (AR: 0.31 ± 0.06, $n = 4$) whereas regions distant from the pipette did not exhibit any alternans (AR: 0.06 ± 0.01, $n = 4$, $P < 0.05$). To exclude any effects caused by pressure ejection itself, control experiments were conducted in which the pipette contained normal Tyrode solution (Fig. 8*D–F*). Under these conditions, regions close to (*a*) and far from (*b*) the pipette tip displayed uniform $[Ca^{2+}]_i$ transients before and after a 20 s pressure application (Fig. 8*E*). Average values from five cells revealed that neither the proximal (filled bar, AR: 0.08 ± 0.01, $n = 5$) nor the distal (open bar, AR: 0.03 ± 0.01, $n = 5$; N.S.) regions showed any Ca^{2+} alternans. Taken together, the present results suggest that spatially restricted subcellular Ca^{2+} alternans can be elicited by local inhibition of glycolysis in the absence of alterations of intracellular pH.

Fructose phosphates, pyruvate and L-lactate exert direct effects on SR Ca^{2+} release

So far, we have shown that extracellular application of the glycolytic products pyruvate or L-lactate to intact atrial myocytes caused acidosis and serious impairment of E–C coupling, i.e. a decrease of AP-induced $[Ca^{2+}]_i$ transients and the generation of Ca^{2+} alternans. Those experiments, however, could not reveal whether pyruvate and L-lactate exerted their effects directly (e.g. via inhibition of Ca^{2+}-induced Ca^{2+} release from the SR) or indirectly (e.g. via intracellular acidosis). To distinguish between these two possibilities, experiments were performed in which the effects of the two glycolytic products on SR Ca^{2+} release could be studied with pH (and [ATP]) kept constant. Two experimental approaches were employed: (1) isolated cardiac RyRs incorporated into lipid bilayers and (2) saponin-permeabilized atrial myocytes. In addition, these experimental approaches allowed us to test for direct effects on SR Ca^{2+} release of other glycolytic intermediates that are not membrane permeant, including glucose-6-phosphate (G6P), fructose-6-phosphate (F6P), fructose-1,6-bisphosphate (FBP), and phosphoenolpyruvate (PEP).

Figure 9 illustrates effects of various intermediates and products of glycolysis on the activity of isolated cardiac RyRs. Figure 9*A* shows original single channel recordings of RyRs under control condition ($cis\,[Ca^{2+}] = 3\ \mu M$) and after addition of 1 mM F6P, FBP, pyruvate and L-lactate. It is evident that FBP significantly increased RyR activity. On average, FBP (1 mM) increased the open probability (P_o) of RyR by $265 \pm 60\%$ ($n = 9$; $P < 0.001$). In contrast, two other sugar phosphates, G6P and F6P, were less effective in stimulating RyRs. G6P and F6P (in both cases 1 mM) increased P_o by $14 \pm 13\%$ ($n = 4$; N.S.) and $39 \pm 9\%$ ($n = 4$; $P < 0.05$), respectively. PEP did not affect RyR activity. Products of glycolysis, however, had opposite effects on RyR activity. Pyruvate (1 mM) decreased P_o of RyR by $58 \pm 10\%$ ($n = 12$; $P < 0.001$). The same concentration of L-lactate did not cause significant inhibition of RyR ($-16 \pm 10\%$; $n = 8$). However, raising

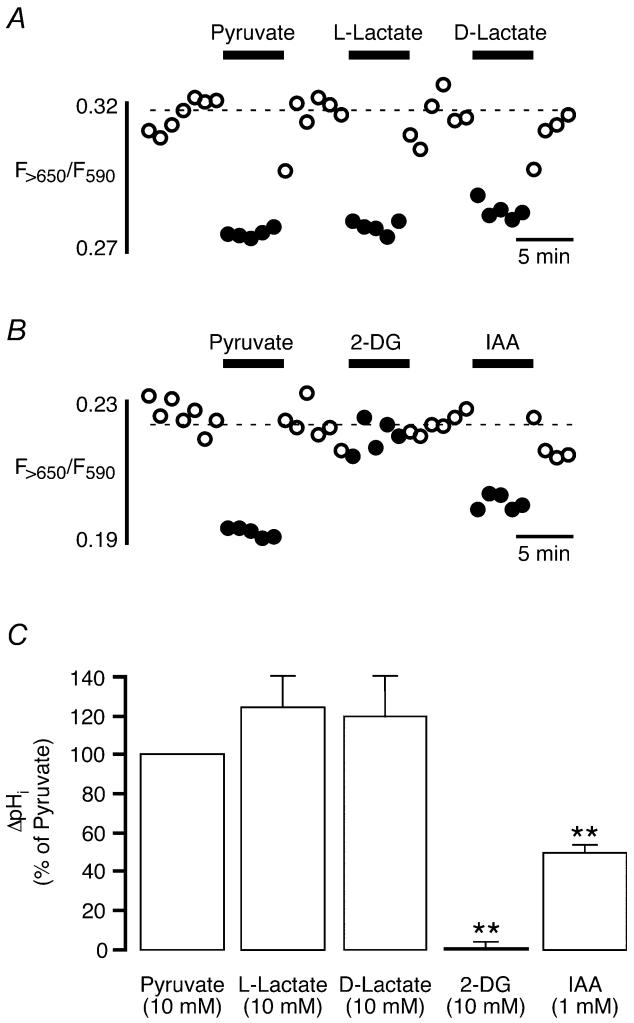

Figure 7. Changes of intracellular pH induced by exposure of atrial myocytes to inhibitiors and products of glycolysis
A and *B*, original recordings of the ratio of carboxy SNARF-1 fluorescence ($F_{>650}/F_{590}$) from two atrial myocytes challenged with pyruvate (10 mM, *A* and *B*), L-lactate (10 mM, *A*), D-lactate (10 mM, *A*), 2-DG (10 mM, *B*), and IAA (1 mM, *B*). Except for 2-DG, all substances tested decreased intracellular pH as indicated by the decrease in fluorescence ratio. *C*, mean values from five (L- and D-lactate) and seven (2-DG and IAA) atrial myocytes. Values are normalized to the initial pH_i decrease induced by 10 mM pyruvate. $^{**}P < 0.01$.

[lactate] to 4 mM decreased P_o by $35 \pm 11\%$ ($n = 6$; $P < 0.05$; data not shown). These data indicate that there is a certain degree of specificity among glycolytic products to inhibit RyRs. All effects of glycolytic compounds on RyR activity were completely reversible (see also Zima *et al.* 2003*b*). Figure 9*B* summarizes the effects of G6P, F6P, FBP, PEP, pyruvate and L-lactate (1 mM for all compounds) on P_o of cardiac RyRs. Thus, the various glycolytic intermediates and products tested exerted distinct inhibitory and stimulatory effects on RyR activity.

To further characterize how intermediates and products of glycolysis might affect SR Ca^{2+} release under more physiological conditions, we tested their effects on spontaneous SR Ca^{2+} release events (Ca^{2+} sparks) in permeabilized atrial myocytes. For this purpose we chose the two substances with the largest stimulatory and inhibitory effects on RyR P_o, FBP and pyruvate, respectively. As illustrated in Fig. 10*A*, application of FBP (1 mM) resulted in a transient increase in the frequency of Ca^{2+} sparks. The frequency increased by $63 \pm 7\%$ ($P < 0.001$) measured after 1 min and by $17 \pm 7\%$ ($P < 0.05$; $n = 7$) after 6 min. Figure 10*B* shows analogous experiments with pyruvate. Contrary to FBP, pyruvate (4 mM) decreased the frequency of Ca^{2+} sparks in permeabilized atrial myocytes to $51 \pm 11\%$ ($P < 0.05$) measured after 2 min of pyruvate application. This inhibitory effect had a tendency to recover to control levels. After 6 min, pyruvate decreased the Ca^{2+} spark frequency to $65 \pm 9\%$ of control ($P < 0.01$; $n = 5$). These results are consistent with the RyR data (Fig. 9) and suggest that FBP (and F6P) can directly stimulate, whereas pyruvate (and L-lactate) can directly inhibit SR Ca^{2+} release through RyRs.

Discussion

Glycolysis has been recognized as an important modulator of E–C coupling in the heart. Previous studies have

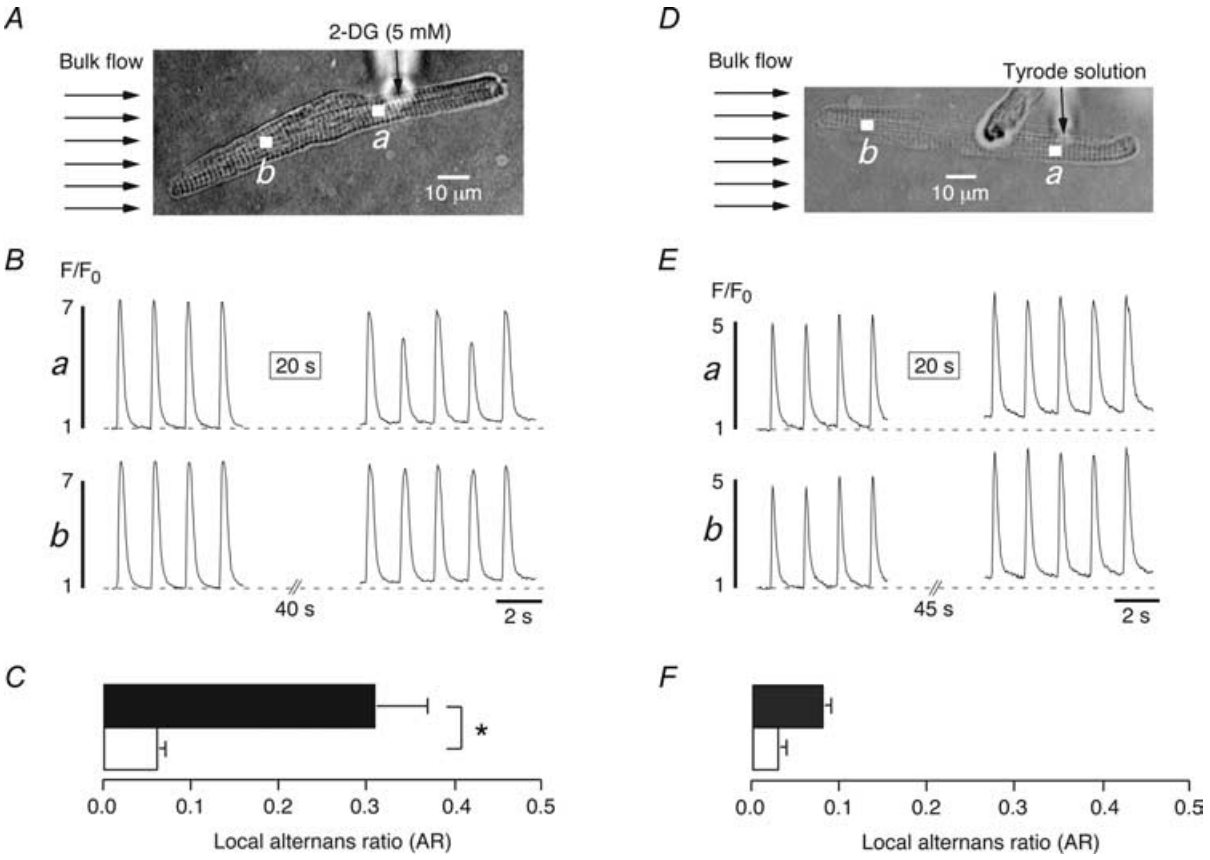

Figure 8. Local inhibition of glycolysis by focal application of 2-deoxy-D-glucose induces locally restricted Ca^{2+} alternans in atrial myocytes

A, focal application of 2-DG (5 mM)-containing Tyrode solution through the tip of a glass micropipette (vertical arrow) to an atrial myocyte. Bulk flow (horizontal arrows) indicates the direction of the laminar superfusion of the cell. *B,* $[Ca^{2+}]_i$ transients from the region close to (*a*) and far from (*b*) the pipette tip as illustrated in *A*. The rectangle (20 s) in trace *a* indicates a 20 s application of the 2-DG-containing Tyrode solution. *C,* mean values of the local alternans ratio (AR) from regions close to (black bar) and far from (white bar) the pipette tip ($n = 5$). *D–F,* analogous control experiments in which the glass pipette contained normal Tyrode solution. Focal application of normal Tyrode solution did not induce any alternans under these conditions. $^*P < 0.05$.

established that some of the ion channels, transporters and pumps involved in E–C coupling are subject to modulation by glycolysis either by glycolytically derived ATP or by intermediates of the glycolytic pathway. The aim of the present study was to characterize in detail the multiple effects exerted by glycolysis on SR Ca^{2+} release in atrial myocytes. Our main findings are: (1) an intact glycolytic pathway is essential for atrial E–C coupling; block of glycolytic enzymes can seriously impair SR Ca^{2+} release without necessarily changing intracellular pH or compromising the overall metabolic (redox) state of the myocytes; (2) inhibition of glycolysis reduces Ca^{2+} sequestration by the SERCA and SR Ca^{2+} load; (3) the glycolytic products pyruvate and L-lactate directly inhibit SR Ca^{2+} release by suppression of RyR activity; and (4) the glycolytic intermediates F6P and FBP directly stimulate SR Ca^{2+} release by increasing the open probability of RyRs. Taken together, the results suggest that glycolysis can exert complex stimulatory and inhibitory effects on SR Ca^{2+} release in atrial myocytes that may include local regulation of ATP, fructose phosphates, pyruvate and L-lactate in the microenvironment of key proteins involved in E–C coupling, particularly RyR and SERCA.

Inhibition of aerobic glycolysis by IAA or 2-DG resulted in elevation of diastolic $[Ca^{2+}]_i$, a decrease of the amplitude of the AP-induced $[Ca^{2+}]_i$ transient, and Ca^{2+} alternans (Fig. 1), demonstrating that the glycolytic pathway acts as a key regulator of atrial SR Ca^{2+} release. Even though IAA and 2-DG caused a small change in the redox state (oxidation) of the mitochondria (Fig. 5), this change did not affect twitch and caffeine-induced $[Ca^{2+}]_i$ transients, indicating that inhibition of glycolysis *per se* did not compromise cellular energy metabolism. The latter finding is consistent with ^{31}P-NMR studies on whole hearts showing that inhibition of aerobic glycolysis by IAA or 2-DG did not seriously affect high-energy phosphate levels (Pirolo & Allen, 1986). Glycolytic enzymes are associated with the sarcolemmal and the SR membranes (Pierce & Philipson, 1985; Han *et al.* 1992; Xu *et al.* 1995). Therefore, the substrates and products of the glycolytic enzymes as well as their cofactors are ideal candidates as modulators of SR function in general, and the RyR and SERCA in particular. Below, we discuss the current evidence for the specific roles of glycolytically derived ATP, glycolytic intermediates and products, and changes of pH_i in the modulation of SR Ca^{2+} release through the cardiac RyR.

Role of glycolytically derived ATP

IAA is a reasonably selective inhibitor of glycolysis, at least in the concentration range studied (0.2–1.0 mM), blocking the glycolytic enzyme GAPDH (Carlson & Siger, 1959). IAA caused acidification of the cytosol (Fig. 7). Thus, both the decrease of pH_i and the inhibition of GAPDH might have contributed to the effects of IAA on electrically evoked $[Ca^{2+}]_i$ transients. 2-DG is a substrate of the sarcolemmal glucose transporter and the glycolytic enzyme hexokinase.

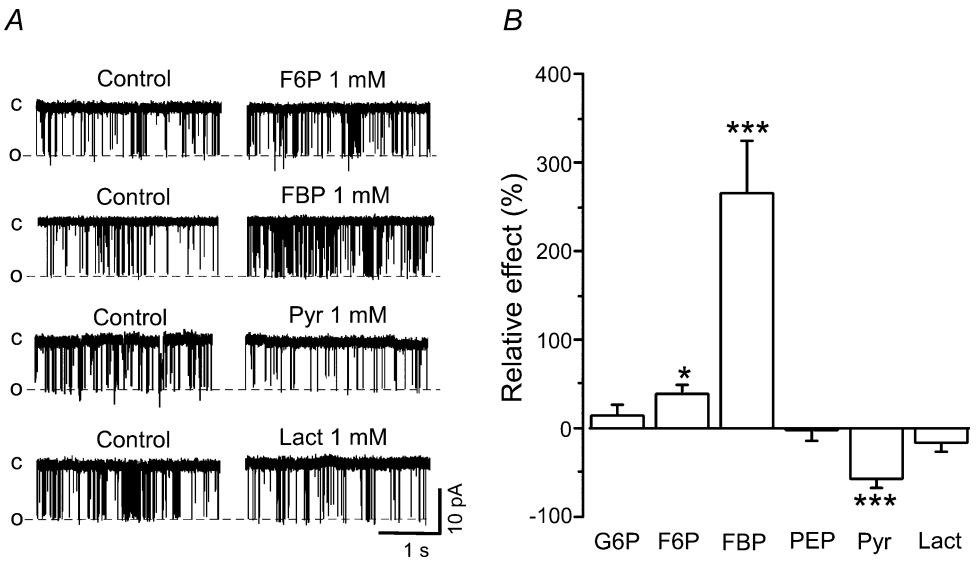

Figure 9. Modulation of ryanodine receptor single channel activity by intermediates and products of glycolysis

A, original single channel recordings of ryanodine receptor (RyR) activity before (Control) and after addition of fructose-6-phosphate (F6P,1 mM), fructose-1,6-bisphosphate (FBP, 1 mM), pyruvate (Pyr, 1 mM), and L-lactate (Lact, 1 mM). c, closed; o, open channel. *B,* mean values of the relative changes of RyR activity (open probability) induced by glucose-6-phosphate (G6P, 1 mM, $n = 4$), F6P ($n = 4$), FBP ($n = 9$), phosphoenolpyruvate (PEP, 1 mM, $n = 4$), Pyr ($n = 12$), and Lact ($n = 8$). $^*P < 0.05$; $^{***}P < 0.001$.

Phosphorylated 2-DG (2-DG-6-P), however, is no longer a substrate of the glycolytic pathway. Thus, like IAA, 2-DG is a selective inhibitor of glycolysis but, in addition, it acts as an effective trap for cytosolic ATP. Previous studies by Allen and colleagues have shown directly that exposure of ferret hearts to 1 mM 2-DG, under aerobic conditions, trapped about 25% of cellular P_i in the form of 2-DG-6-P and reduced cellular ATP concentrations by roughly 30% (Allen *et al.* 1985; Pirolo & Allen, 1986). Unlike IAA, however, inhibition of aerobic glycolysis by 2-DG did not change intracellular pH (Fig. 7) consistent with previous results (Allen *et al.* 1985). Therefore, the changes of E–C coupling elicited by 2-DG were pH independent and, most likely, caused solely by inhibition of glycolytic flux and reduction of cytosolic ATP levels.

Interestingly, when aerobic glycolysis was inhibited in ferret hearts by 0.1 mM IAA, a concentration causing almost complete block of glycolysis, there was no detectable change in either high-energy phosphates or cardiac function (Pirolo & Allen, 1986). This finding

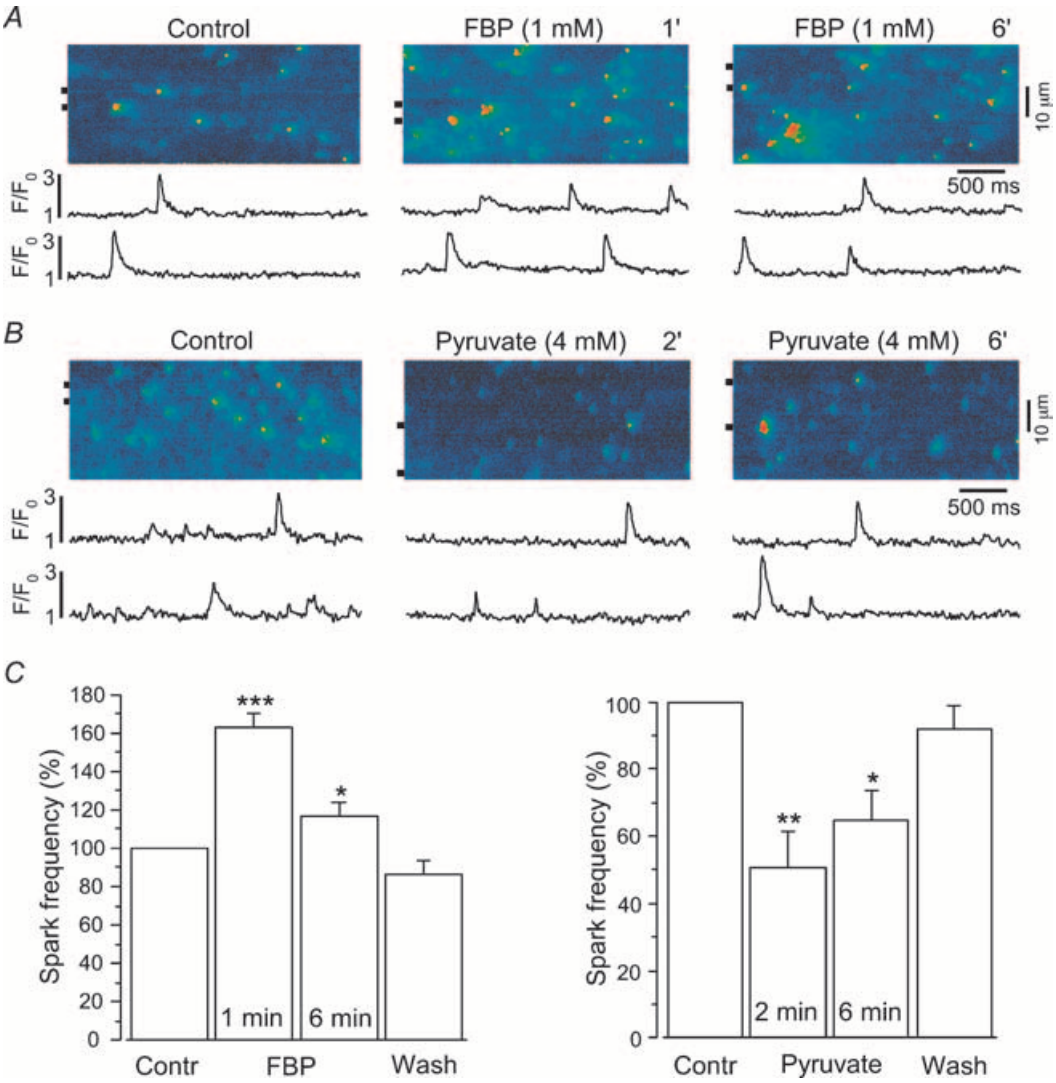

Figure 10. Effects of fructose-1,6-bisphosphate (FBP) and pyruvate on the frequency of spontaneous Ca^{2+} sparks in saponin-permeabilized atrial myocytes

A and *B,* original linescan images of Ca^{2+} spark activity in two permeabilized atrial myocytes before (Control) and after addition of FBP (1 mM, *A*) or pyruvate (4 mM, B). Compared to intact cell experiments (Fig. 6), [pyruvate] was reduced to 4 mM to achieve approximately the same effective cytosolic concentration. Pyruvate has been shown to reach intracellular levels of about a third of the extracellular [pyruvate] in whole heart experiments (Mallet & Sun, 1999). Traces below the linescan images show normalized (F/F_0) local fluorescence changes of the regions marked by the horizontal lines next to the images. FBP increased, whereas pyruvate decreased, Ca^{2+} spark activity. *C,* mean values of spark frequencies recorded before (Contr), during, and following washout (Wash) of FBP (left panel, $n = 7$) or pyruvate (right panel, $n = 5$). $^*P < 0.05$; $^{**}P < 0.01$; $^{***}P < 0.001$.

suggests that under aerobic conditions glycolysis produces only a minimal fraction of total cellular ATP. Still, IAA was able to induce serious impairment of the electrically evoked $[Ca^{2+}]_i$ transient in our experiments, implying that locally restricted decreases of glycolytically derived ATP – undetectable at the bulk cellular level – might be able to affect SR Ca^{2+} release. This notion is supported by experiments showing that focally applied IAA (0.2 mM, Kockskämper & Blatter, 2002) or 2-DG (5 mM, this study, Fig. 8) caused local Ca^{2+} alternans that was confined to the subcellular region of exposure.

In conclusion, the results obtained with the glycolytic inhibitors suggest (1) that glycolysis is important for maintaining atrial E–C coupling and (2) that inhibition of glycolysis (by either IAA or 2-DG) causes impairment of the $[Ca^{2+}]_i$ transient in part by reducing the amount of glycolytically derived ATP in the microenvironment of the RyR and SERCA.

Nevertheless, we also considered the possibility that membrane currents relevant to E–C coupling could play a role in the observed changes of Ca^{2+} release and SR Ca^{2+} load. In whole-cell voltage clamp experiments we observed (data not shown) that neither IAA nor pyruvate significantly altered peak L-type Ca^{2+} current (see also Hüser *et al.* 2000), suggesting that the observed decrease in $[Ca^{2+}]_i$ transient amplitude (Fig. 1) was unlikely to be the result of a reduced trigger for Ca^{2+}-induced Ca^{2+} release. Furthermore, glibenclamide (20 μM), a potent inhibitor of the ATP-dependent potassium current ($I_{K,ATP}$) in atrial myocytes (Wang & Lipsius, 1995), did not change the effects of IAA on $[Ca^{2+}]_i$ transient amplitude and SR Ca^{2+} load (data not shown). Therefore, changes in ATP-dependent K^+ conductance and $I_{K,ATP}$-induced changes in AP configuration are unlikely to account for the observations made in this study, even though severe metabolic impairment in conjunction with hypoxic conditions can affect AP configuration in atrial tissue (e.g. Senges *et al.* 1981).

Role of acidosis

Intracellular pH is an important modulator of cardiac function. Acidosis has been shown (1) to elevate diastolic $[Ca^{2+}]_i$ (Kohmoto *et al.* 1990), (2) to change the amplitude and the kinetics of the $[Ca^{2+}]_i$ transient (Kohmoto *et al.* 1990; Choi *et al.* 2000), and (3) to cause alternans (Orchard *et al.* 1991; Diaz *et al.* 2002). Since many of the inhibitors and products of glycolysis tested in this study (IAA, pyruvate, lactate) caused similar changes of $[Ca^{2+}]_i$ along with intracellular acidosis, it is likely that the reduction of pH_i contributed to the observed alterations of Ca^{2+} homeostasis. However, as pointed out above, the same changes could also be induced by inhibition of glycolysis (using 2-DG) when pH_i was essentially unchanged indicating that acidosis is not a prerequisite for the observed alterations of Ca^{2+} homeostasis and that other factors may be even more important for the modulation of SR Ca^{2+} release by glycolysis (e.g. local [ATP]).

The effects of pyruvate and lactate on Ca^{2+} handling in ventricular myocardium have been studied in considerable detail before (e.g. Allen *et al.* 1989; Cairns *et al.* 1993; Terracciano & MacLeod, 1997; Martin *et al.* 1998; Hüser *et al.* 2000; Hasenfuss *et al.* 2002; Zima *et al.* 2003*b*). Both pyruvate and lactate exert complex effects on $[Ca^{2+}]_i$ consisting of an elevation of diastolic $[Ca^{2+}]_i$, the induction of Ca^{2+} alternans, a slowing of the kinetics and changes in the amplitude of the $[Ca^{2+}]_i$ transient. Some of these effects have been attributed to intracellular acidification. In line with this notion we found that pyruvate and lactate caused the same degree of intracellular acidification in atrial myocytes (Fig. 7). Importantly, however, not all of the effects of the glycolytic products can be explained solely on the basis of intracellular acidification. For example, in rat ventricular myocytes it has been shown that the increase of the $[Ca^{2+}]_i$ transient (and contractions) induced by pyruvate was mediated, in part, by stimulation of mitochondrial metabolism (Martin *et al.* 1998; Zima *et al.* 2003*b*). Furthermore, part of the pyruvate-mediated alterations of the $[Ca^{2+}]_i$ transient could be attributed to direct modulation of the activity of the RyR (Zima *et al.* 2003*b*). The latter observation in conjunction with a previous study (Kermode *et al.* 1998) prompted us to investigate possible direct effects of intermediates and products of glycolysis on RyR activity.

Direct modulation of SR Ca^{2+} release by intermediates and products of glycolysis

Our results indicate that SR Ca^{2+} release in cardiac myocytes is subject to direct stimulation and inhibition, respectively, by intermediates and products of glycolysis (Fig. 9). F6P and FBP stimulated RyR activity. By contrast, pyruvate and L-lactate inhibited RyR activity. Modulation of RyR activity by sugar phosphates of the glycolytic pathway has been demonstrated before (Kermode *et al.* 1998). Although the relative potencies of G6P, F6P and FBP varied somewhat, there is general agreement between the two studies that the sugar phosphates stimulate RyR activity with FBP being the most potent and efficacious of the glycolytic intermediates. The modulation of RyR activity observed in lipid bilayer recordings also occurred in isolated permeabilized atrial myocytes. FBP decreased and pyruvate increased the frequency of spontaneous SR Ca^{2+} release events (Ca^{2+} sparks, Fig. 10), in line with the data obtained from isolated RyRs. Thus, the modulation of RyR activity measured in an isolated system (planar lipid bilayer) was also present under more physiological conditions in a cellular system with intact SR function,

indicating that this kind of direct modulation of SR Ca^{2+} release is of physiological relevance.

It is important to note that glycolytically induced changes of RyR activity alone are not sufficient to account for the observed steady-state changes of the $[Ca^{2+}]_i$ transient. As pointed out previously, increasing or decreasing the open probability of the RyR affects $[Ca^{2+}]_i$ transient amplitude only transiently (Trafford *et al.* 2002). For steady-state changes to occur, SR Ca^{2+} load has to change accordingly, which may require that the activity of the SERCA is also affected by inhibition of glycolysis. Several factors argue in favour of this hypothesis. First, the SR Ca^{2+} pump is preferentially fuelled by glycolytic ATP (Xu *et al.* 1995). Second, our experiments show that block of glycolysis causes a 15–20% reduction of SR Ca^{2+} content (see Fig. 2), although this may be an underestimation because of the non-linear relationship between fluo-4 fluorescence and $[Ca^{2+}]$. Third, the activity of the SERCA was reduced in the presence of IAA or 2-DG (Figs 3 and 4), presumably as a result of reduced levels of glycolytically derived ATP. SR content is not only critically dependent on absolute ATP levels, but also on the ratio of [ATP] to [ADP] (Zima *et al.* 2003*b*; for review see Kodama, 1985), consistent with the notion that increased [ADP] alters SR Ca^{2+} handling properties and decreases the SR Ca^{2+} capacity (Macdonald & Stephenson, 2004). Thus, the reduction of SR Ca^{2+} content represents yet another mechanism contributing to the changes of the $[Ca^{2+}]_i$ transient observed during inhibition of glycolysis.

Physiological and pathophysiological implications

The present study revealed a complex modulation of atrial E–C coupling by glycolysis. According to our results, glycolysis may modulate SR Ca^{2+} release locally by direct and indirect mechanisms including modulation of RyR activity by intermediates and products of glycolysis as well as local changes of glycolytically derived ATP (which also affects SERCA activity) or changes of pH_i. Interestingly, sugar phosphates appearing early in the glycolytic pathway stimulated whereas products of glycolysis inhibited RyR activity. Thus, a delicate balance may exist between local changes of pH_i, ATP, fructose phosphates, pyruvate and L-lactate in modulating the activity of the cardiac RyR and consequently the magnitude of SR Ca^{2+} release. The situation becomes even more complex considering that changes of local [ATP] may not only modulate RyR function directly but also indirectly through changes of phosphorylation potential and Mg^{2+} (Fill & Copello, 2002). Furthermore, the cardiac RyR is also modulated by cytosolic NAD^+ and NADH. NADH inhibits RyR activity and SR Ca^{2+} release and this inhibition is relieved by NAD^+ (Zima *et al.* 2003*a*, 2004). Since these adenine dinucleotides are cofactors of two key enzymes of the glycolytic pathway, GAPDH and lactate dehydrogenase, regulation of the cytosolic NADH/NAD^+ ratio represents still another means by which glycolysis can modulate cardiac SR Ca^{2+} release. Thus, any perturbation eliciting only subtle changes of glycolytic flux may, in principle, modulate SR Ca^{2+} release and E–C coupling. At any given time the balance between local changes in the concentrations of stimulatory and inhibitory modulators of the RyR will decide about changes of its open probability. An important pathophysiological example is ischaemia. During ischaemia, the concentrations of inhibitors of RyR activity rise dramatically (L-lactate, H^+, NADH, Mg^{2+}) whereas, at the same time, the concentrations of stimulators of RyR activity decrease (ATP, NAD^+). The overall result will be decreased activity of the RyR contributing to the suppression of $[Ca^{2+}]_i$ transients during ischaemia. Finally, the results of this study may also be relevant to heart failure. In heart failure, transporters and enzymes involved in glycolysis are down-regulated (reviewed in Ventura-Clapier *et al.* 2003) suggesting that altered glycolytic flux may also contribute to abnormal Ca^{2+} handling and release in the failing heart.

References

Allen DG, Lee JA & Smith GL (1989). The consequences of simulated ischaemia on intracellular Ca^{2+} and tension in isolated ferret ventricular muscle. *J Physiol* **410**, 297–323.

Allen DG, Morris PG, Orchard CH & Pirolo JS (1985). A nuclear magnetic resonance study of metabolism in the ferret heart during hypoxia and inhibition of glycolysis. *J Physiol* **361**, 185–204.

Bassani JW, Bassani RA & Bers DM (1994). Relaxation in rabbit and rat cardiac cells: species-dependent differences in cellular mechanisms. *J Physiol* **476**, 279–293.

Bers DM (2001). *Excitation-Contraction Coupling and Cardiac Contractile Force*, 2nd edn. Kluwer Academic Publishers, Dordrecht, Netherlands.

Cairns SP, Westerblad H & Allen DG (1993). Changes in myoplasmic pH and calcium concentration during exposure to lactate in isolated rat ventricular myocytes. *J Physiol* **464**, 561–574.

Carlson FD & Siger A (1959). The creatine phosphotransfer reaction in iodoacetate-poisoned muscle. *J General Physiol* **43**, 301–313.

Choi HS, Trafford AW, Orchard CH & Eisner DA (2000). The effect of acidosis on systolic Ca^{2+} and sarcoplasmic reticulum calcium content in isolated rat ventricular myocytes. *J Physiol* **529**, 661–668.

Diaz ME, Eisner DA & O'Neill SC (2002). Depressed ryanodine receptor activity increases variability and duration of the systolic Ca^{2+} transient in rat ventricular myocytes. *Circ Res* **91**, 585–593.

Diaz ME, O'Neill SC & Eisner DA (2004). Sarcoplasmic reticulum calcium content fluctuation is the key to cardiac alternans. *Circ Res* **94**, 650–656.

Elliott AC, Smith GL, Eisner DA & Allen DG (1992). Metabolic changes during ischaemia and their role in contractile failure in isolated ferret hearts. *J Physiol* **454**, 467–490.

Fill M & Copello JA (2002). Ryanodine receptor calcium release channels. *Physiol Rev* **82**, 893–922.

Glitsch HG & Tappe A (1993). The Na^+/K^+ pump of cardiac Purkinje cells is preferentially fuelled by glycolytic ATP production. *Pflugers Arch* **422**, 380–385.

Han JW, Thieleczek R, Varsanyi M & Heilmeyer LM Jr (1992). Compartmentalized ATP synthesis in skeletal muscle triads. *Biochemistry* **31**, 377–384.

Hasenfuss G, Maier LS, Hermann HP, Lüers C, Hünlich M, Zeitz O, Janssen PM & Pieske B (2002). Influence of pyruvate on contractile performance and Ca^{2+} cycling in isolated failing human myocardium. *Circulation* **105**, 194–199.

Hüser J, Wang YG, Sheehan KA, Cifuentes F, Lipsius SL & Blatter LA (2000). Functional coupling between glycolysis and excitation-contraction coupling underlies alternans in cat heart cells. *J Physiol* **524**, 795–806.

Kermode H, Chan WM, Williams AJ & Sitsapesan R (1998). Glycolytic pathway intermediates activate cardiac ryanodine receptors. *FEBS Lett* **431**, 59–62.

Kockskämper J & Blatter LA (2002). Subcellular Ca^{2+} alternans represents a novel mechanism for the generation of arrhythmogenic Ca^{2+} waves in cat atrial myocytes. *J Physiol* **545**, 65–79.

Kockskämper J, Sheehan KA, Bare DJ, Lipsius SL, Mignery GA & Blatter LA (2001). Activation and propagation of Ca^{2+} release during excitation-contraction coupling in atrial myocytes. *Biophys J* **81**, 2590–2605.

Kodama T (1985). Thermodynamic analysis of muscle ATPase mechanisms. *Physiol Rev* **65**, 467–551.

Kohlhardt M, Fichtner H & Fröbe U (1989). Metabolites of the glycolytic pathway modulate the activity of single cardiac Na^+ channels. *FASEB J* **3**, 1963–1967.

Kohmoto O, Spitzer KW, Movsesian MA & Barry WH (1990). Effects of intracellular acidosis on $[Ca^{2+}]_i$ transients, transsarcolemmal Ca^{2+} fluxes, and contraction in ventricular myocytes. *Circ Res* **66**, 622–632.

Losito VA, Tsushima RG, Diaz RJ, Wilson GJ & Backx PH (1998). Preferential regulation of rabbit cardiac L-type Ca^{2+} current by glycolytic derived ATP via a direct allosteric pathway. *J Physiol* **511**, 67–78.

Macdonald WA & Stephenson DG (2004). Effects of ADP on action potential-induced force responses in mechanically skinned rat fast-twitch fibres. *J Physiol* **559**, 433–447.

Mallet RT & Sun J (1999). Mitochondrial metabolism of pyruvate is required for its enhancement of cardiac function and energetics. *Cardiovasc Res* **42**, 149–161.

Martin BJ, Valdivia HH, Bünger R, Lasley RD & Mentzer RM Jr (1998). Pyruvate augments calcium transients and cell shortening in rat ventricular myocytes. *Am J Physiol* **274**, H8–H17.

Mejia-Alvarez R & Marban E (1992). Mechanism of the increase in intracellular sodium during metabolic inhibition: direct evidence against mediation by voltage-dependent sodium channels. *J Mol Cell Cardiol* **24**, 1307–1320.

O'Rourke B, Ramza BM & Marban E (1994). Oscillations of membrane current and excitability driven by metabolic oscillations in heart cells. *Science* **265**, 962–966.

Opie LH (1995). Substrate and energy metabolism of the heart. In *Physiology and Pathophysiology of the Heart*, 3rd edn, ed. Sperelakis N, pp. 385–411. Kluwer Academic Publishers, Dordrecht, Netherlands.

Orchard CH, McCall E, Kirby MS & Boyett MR (1991). Mechanical alternans during acidosis in ferret heart muscle. *Circ Res* **68**, 69–76.

Pierce GN & Philipson KD (1985). Binding of glycolytic enzymes to cardiac sarcolemmal and sarcoplasmic reticular membranes. *J Biol Chem* **260**, 6862–6870.

Pirolo JS & Allen DG (1986). Assessment of techniques for preventing glycolysis in cardiac muscle. *Cardiovasc Res* **20**, 837–844.

Poole RC & Halestrap AP (1993). Transport of lactate and other monocarboxylates across mammalian plasma membranes. *Am J Physiol* **264**, C761–C782.

Romashko DN, Marban E & O'Rourke B (1998). Subcellular metabolic transients and mitochondrial redox waves in heart cells. *Proc Natl Acad Sci U S A* **95**, 1618–1623.

Senges J, Brachmann J, Pelzer D, Rizos I & Kübler W (1981). Effect of glycolytic inhibitors on the sinoatrial node, atrium and atrioventricular node in the rabbit heart. *J Mol Cell Cardiol* **13**, 811–821.

Sugiyama S, Satoh H, Nomura N, Terada H, Watanabe H & Hayashi H (2001). The importance of glycolytically-derived ATP for the Na^+/H^+ exchange activity in guinea pig ventricular myocytes. *Mol Cell Biochem* **217**, 153–161.

Terracciano CMN & MacLeod KT (1997). Effects of lactate on the relative contribution of Ca^{2+} extrusion mechanisms to relaxation in guinea-pig ventricular myocytes. *J Physiol* **500**, 557–570.

Trafford AW, Diaz ME, O'Neill SC & Eisner DA (2002). Integrative analysis of calcium signalling in cardiac muscle. *Front Biosci* **7**, d843–852.

Ventura-Clapier R, Garnier A & Veksler V (2003). Energy metabolism in heart failure. *J Physiol* **555**, 1–13.

Wang YG & Lipsius SL (1995). Acetylcholine activates a glibenclamide-sensitive K^+ current in cat atrial myocytes. *Am J Physiol* **268**, H1322–H1334.

Weiss JN & Lamp ST (1987). Glycolysis preferentially inhibits ATP-sensitive K^+ channels in isolated guinea pig cardiac myocytes. *Science* **238**, 67–69.

Weiss JN & Lamp ST (1989). Cardiac ATP-sensitive K^+ channels. Evidence for preferential regulation by glycolysis. *J General Physiol* **94**, 911–935.

Wu M-L & Vaughan-Jones RD (1994). Effect of metabolic inhibitors and second messengers upon Na^+-H^+ exchange in the sheep cardiac Purkinje fibre. *J Physiol* **478**, 301–313.

Wu J, Vereecke J, Carmeliet E & Lipsius SL (1991). Ionic currents activated during hyperpolarization of single right atrial myocytes from cat heart. *Circ Res* **68**, 1059–1069.

Xu KY, Zweier JL & Becker LC (1995). Functional coupling between glycolysis and sarcoplasmic reticulum Ca^{2+} transport. *Circ Res* **77**, 88–97.

Zima AV, Copello JA & Blatter LA (2003*a*). Differential modulation of cardiac and skeletal muscle ryanodine receptors by NADH. *FEBS Lett* **547**, 32–36.

Zima AV, Copello JA & Blatter LA (2004). Effects of cytosolic NADH/NAD^+ levels on sarcoplasmic reticulum Ca^{2+} release in permeabilized rat ventricular myocytes. *J Physiol* **555**, 727–741.

Zima AV, Kockskämper J, Mejia-Alvarez R & Blatter LA (2003*b*). Pyruvate modulates cardiac sarcoplasmic reticulum Ca^{2+} release in rats via mitochondria-dependent and independent mechanisms. *J Physiol* **550**, 765–783.

Acknowledgements

This work was supported by the NIH (NIH R01HL62231 to L.A.B.) and the Potts Estate, Loyola University Chicago (RFC 107457 to A.V.Z.). J.K. was a recipient of fellowships from the Falk Foundation (Loyola University Chicago) and the Deutsche Forschungsgemeinschaft (DFG).

Author's present address

J. Kockskämper: Abteilung Kardiologie und Pneumologie, Georg-August-Universität, Robert-Koch-Str. 40, 37075 Göttingen, Germany.